C. elegans PVF-1 inhibits permissive UNC-40 signalling through CED-10 GTPase to position the male ray 1 sensillum

Gratien Dalpe[1], Marina Tarsitano[2,*], M. Graziella Persico[2,‡], Hong Zheng[1] and Joseph Culotti[1,3,§]

SUMMARY

Graded distributions of netrin and semaphorin guidance cues convey instructive polarity information to migrating cells and growth cones, but also have permissive (i.e. non-polarity determining) functions in mammalian development and repair. The permissive functions of these cues are largely uncharacterised at a molecular level. We found previously that UNC-6 (netrin) signals permissively through UNC-40 (DCC) and UNC-5 receptors to prevent anterior displacement of the ray 1 sensillum in the *C. elegans* male tail. UNC-6/UNC-40 signalling functions in parallel with SMP-1 (semaporin 1)/PLX-1 (plexin) signalling to prevent this defect. Here, we report that a deletion allele of *pvf-1*, which encodes a VEGF-related protein, causes no ray 1 defects, but enhances ray 1 defects of a *plx-1* mutant, and unexpectedly also suppresses *unc-6(ev400)*-null mutant ray 1 defects. These mutant ray 1 inductive and suppressive effects are mimicked by the ability of *unc-40(+)* and *ced-10(gain-of-function)* multi-copy transgene arrays to induce ray 1 defects or suppress *unc-6* mutant ray 1 defects, depending on their dosage, suggesting the *pvf-1* mutation causes UNC-40 overactivity that interferes with signalling but is partially sensitive to UNC-6. Additional data suggest PVF-1 functions through four VEGF receptor-related proteins and inhibits only CED-10 (a GTPase), but not MIG-2-dependent UNC-40 activity, even though UNC-40 functions through both GTPases to position ray 1. *pvf-1* and receptor mutant ray 1 defects are rescued by transgenes expressing mouse VEGF164 and human VEGF receptors, respectively. These data report the first case of VEGF-induced inhibition of the netrin signalling and a molecular conservation of VEGF function from worms to humans.

KEY WORDS: PVF-1/VEGF, UNC-40/DCC, GTPase, Crosstalk

INTRODUCTION

Netrins and semaphorins were discovered as axon guidance cues that instruct the direction of cell movement and axon extension by forming an extracellular gradient that provides polarity information to the migrating cell or axon growth cone. For example, UNC-6 (netrin) is expressed ventrally in *C. elegans* and is graded along the D/V axis of the body wall (Ishii et al., 1992; Wadsworth et al., 1996). Attractive cell and growth cone responses to ventral sources of UNC-6 are mediated by the UNC-40 (DCC) receptor, whereas repulsive responses to UNC-6 are mediated by UNC-40-independent and UNC-40-dependent UNC-5 receptors (Hedgecock et al., 1990; Leung-Hagesteijn et al., 1992; Chan et al., 1996; Merz et al., 2001). Since these discoveries, homologues of these *C. elegans* genes were found to be required instructively (i.e. act as part of a spatially distributed guidance cue gradient) for guiding growth cone migrations in the vertebrate spinal cord and elsewhere in the vertebrate nervous system (Keino-Masu et al., 1996; Serafini et al., 1996; Ackerman et al., 1997; Leonardo et al., 1997).

The semaphorins and their plexin receptors also function as instructive axon guidance cues in a variety of animals (Kolodkin et al., 1992; Kolodkin et al., 1993; Luo et al., 1993). The *C. elegans* genome contains two semaphorin 1 genes, *smp-1* and *smp-2*, and a

single semaphorin 2a gene, *mab-20/smp-3* (Wormbase release WR 237, http://www.wormbase.org). The *C. elegans* genome also encodes two plexins: PLX-1 mediates responses to SMP-1 and SMP-2, whereas PLX-2 mediates responses to MAB-20/SMP-3. There are no neuropilin genes in *C. elegans* (Wormbase release WR 237, http://www.wormbase.org).

Although the netrin and semaphorin families of secreted proteins were originally characterised in the nervous system where they function instructively to guide axons (Tessier-Lavigne et al., 1988), they are also expressed outside the nervous system where they orchestrate the development of several vertebrate organs and tissues, including the vasculature, by regulating cell adhesion, motility, differentiation and survival. Netrins and semaphorins mediate processes that do not obviously involve polarised cell movements and are therefore believed to be purely permissive (i.e. not required to provide polarity information to guide cell movements) (Hinck, 2004; Lai Wing Sun et al., 2011). As observed for axon guidance in the nervous system, netrins and semaphorins may act as bi-functional agents in angiogenesis, based on separate reports that they can have pro-angiogenic (including attractive) (Park et al., 2004; Nguyen and Cai, 2006; Wilson et al., 2006) or anti-angiogenic (including repulsive) (Lu et al., 2004; Larrivée et al., 2007; Bouvrée et al., 2008; Lejmi et al., 2008) actions on endothelial cells.

The finding that netrins can have dual angiogenic and anti-angiogenic properties, whereas VEGFs have pro-angiogenic properties raises the possibility that Netrins are regulated by VEGFs or vice versa. Although VEGF is reported to regulate an HLX transcription factor required for induction of UNC-5B, PLX-A1 and SEMA3G (Testori et al., 2011), all of which inhibit blood vessel sprouting – the first via its activation by netrin 1 (Lu et al., 2004; Larrivée et al., 2007; Bouvrée et al., 2008; Lejmi et al., 2008), we are unaware of any other published regulation of Netrin signalling by VEGF.

[1]Samuel Lunenfeld Research Institute of Mount Sinai Hospital, Toronto, Ontario, M5G 1X5, Canada. [2]Institute of Genetics and Biophysics, CNR, Naples, Italy. [3]Department of Molecular Biology, University of Toronto, Toronto, Ontario, M5S 1SA, Canada.

*Present address: Medical Genetics Services, Cardarelli Hospital, via Carderelli 9, 80131, Naples, Italy
‡Deceased
§Author for correspondence (culotti@lunenfeld.ca)

To investigate the use of *C. elegans* as a model genetic system for revealing interactions between netrin, semaphorin and VEGF signalling in a permissive context, we decided to examine the effects of these cues on the stereotypic patterning of the ray sensillae in the male tail (Dalpé et al., 2004; Dalpé et al., 2012). The nine rays on each side of the male tail are used to sense the hermaphrodite for copulation (Sulston et al., 1980) (Fig. 1A). Each ray sensillum comprises sensory endings from two neurons encircled by the

Fig. 1. Male tail ray sensillae, their development and positioning. Posterior is towards the right in all panels. (**A,B**) Ventral view of a wild-type and a mutant male tail showing the nine finger-like cuticle-lined rays protruding from each side. Rays 1 and 2 are indicated by black and white arrowheads, respectively. All the rays are posterior to the anterior limit of the cuticular fan (arrow) in the wild type, but multiple mutant alleles of *unc-73*, *smp-1*, *plx-1*, *unc-6* and *unc-40* have a severe ray 1 defect in which ray 1 is anterior to the anterior limit of the fan (arrow) (Dalpé et al., 2004; Dalpé et al., 2012) (R. Allore, personal communication). (**C**) Shown is the Rn sublineage division pattern that generates the two neurons RnA (orange) and RnB (red) plus the RnSt ray glial support cell (green) and the Rn.p hypodermal (SET/hyp) cell (yellow) that make up each ray. (**D**) The components of ray 1 colour coded as in C. Other rays also comprise two neurons and a support cell (not shown), as for ray 1. Only the most anterior six rays on one side are represented in this diagram of a lateral perspective. The cuticular fan is shaded light grey. (**E**) Development of the rays starts with the generation of the neurons plus a support cell as a three-cell cluster (derived from a single Rn cell). Most of the clusters are arranged along the A/P axis just ventral to the lateral hypodermal Rn.p cells that make up the lateral seam of the tail (SET). In stage 1 of male development there are no gaps that separate the ray clusters, but gaps appear in stage 2 (Emmons, 2005). In the mutants with ray 1 anterior defects, ray 1, instead of being localised between Rn.1 and Rn.2, is frequently mislocalised to the anterior end of Rn.1 and its junction with the lateral seam (position of blue arrow). Scale bar: 50 μm.

expanded tip of a structural support cell. The support cell and neuron endings are embedded in the fan (a lateral cuticular specialisation made by the hypodermis/epidermis), such that most ray neuron endings protrude through the support cell and the edges of the fan in a characteristic position within a roughly linear A/P oriented array of these sensillae, with ray 1 most anterior and ray 9 most posterior on each side (Fig. 1A,D).

The two neurons and single support cell of each ray derive from a common Rn blast cell and cluster together sublaterally to form a ray precursor (Fig. 1C,E) (Emmons, 2005). Initially, there is contact between neighbouring three-cell clusters. They then separate into distinct ray precursors. For ray 1, this involves an apparent limited movement of the ray 1 cluster towards the anterior relative to ray 2.

We reported previously that two signalling pathways, SMP-1/PLX-1 and UNC-6/UNC-40, function together to prevent the anterior displacement of ray 1 (Fig. 1B) and that together these two pathways can account for all of this function (Dalpé et al., 2004; Dalpé et al., 2012). Although during ray positioning, fluorescently tagged functional versions of SMP-1 (semaphorin 1a) and PLX-1 (plexin) appear expressed in all ray cells, whereas UNC-40 and UNC-6 are expressed and localised, respectively, to ray structural cells, we previously found that both PLX-1 and UNC-40 function in the ray structural cells to prevent ray 1 displacement (Dalpé et al., 2004; Dalpé et al., 2012).

Several lines of evidence suggested that SMP-1 and UNC-6 signal permissively and not instructively in this context (Dalpé et al., 2012). For example, *unc-40(+)* multi-copy arrays, which putatively overexpress UNC-40, can rescue the ray 1 positioning defects of an *unc-6* null mutant, as can heat shock-induced expression of UNC-6 in all cells of *unc-6* mutant animals (Dalpé et al., 2012). Here, we present data suggesting that UNC-40 signalling through the CED-10 Rho family GTPase in this permissive context is normally inhibited by VEGF signalling. Furthermore, mammalian VEGF164 and human VEGF receptors can functionally substitute for their *C. elegans* homologues to position ray 1, demonstrating a high conservation of function at a molecular level. These findings represent the first indication of a VEGF-mediated inhibition of netrin signalling in any animal and raise the possibility that similar crosstalk may be involved in permissive activities of netrins in mammals – activities that could include one or more functions in blood vessel formation. The characterisation of permissive UNC-6, semaphorin and VEGF signalling in a genetically amenable context could shed light on a number of vertebrate processes that are important to development, regeneration and health.

MATERIALS AND METHODS
Nematode culture
General procedures were used for culture, maintenance and storage of *C. elegans* (Wood, 1988). Strains used in this study were: Linkage Group X (LGX), *unc-6(ev400)* (Hedgecock et al., 1990); *ver-4(ok1079)ver-3(gk227)* (Popovici et al., 2002); *mig-2(mu28)* (Zipkin et al., 1997); LGI, *unc-40(e1430)* (Hedgecock et al., 1990); LGIII, *ver-1(ok1738);ver-2(ok897)* (Popovici et al., 2002); *pvf-1(ev763)* (this paper); IV, *ced-10(n1993)* (Ellis et al., 1991); *plx-1(ev724)* (Dalpé et al., 2004); *unc-5(e53)* (Hedgecock et al., 1990); and LGV, *him-5(e1490)* (Hodgkin and Brenner, 1977). Strains not isolated in our laboratory were obtained from the *C. elegans* knockout consortium courtesy of Dr Y. Goshima (Yokohama City University, Japan), from the *C. elegans* Genetics Center courtesy of T. Stiernagle (University of Minnesota, MN, USA) or from Dr Regine Roubin (Institute of Cancer Research, Marseilles, France).

Immunohistochemistry
him-5(e1490) mutant animals were co-transformed with plasmid DNA from vector L4687 (*pPD133.97* – encoding *myo-3p::yfp*) and with *pvf-1p::pvf-*
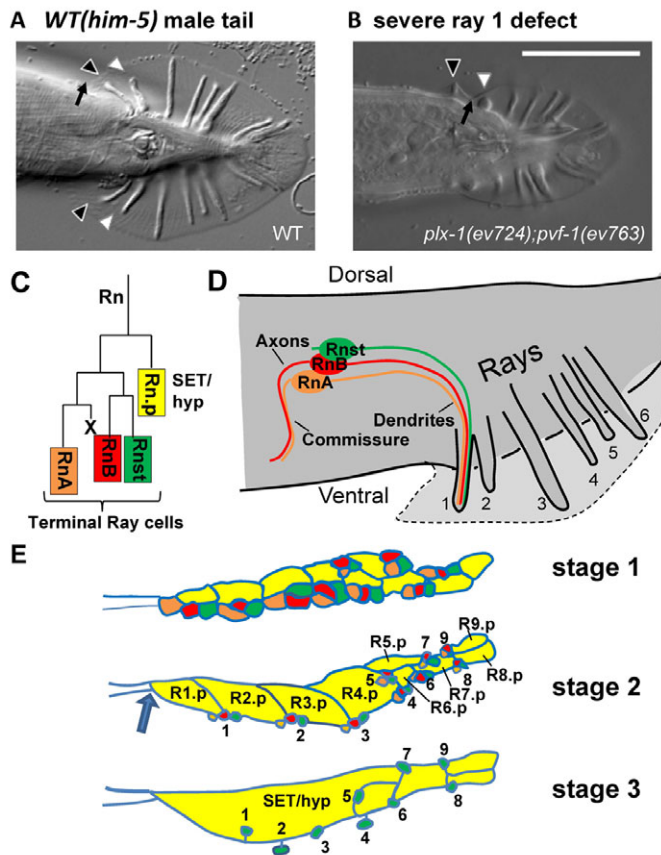
1(+) construct PVL95 (which rescues the *pvf-1* mutant) were permeabilised, fixed and stained using a modified Finney-Ruvkun procedure (Bettinger et al., 1996). The worms were then incubated overnight with 300 ng/µl of a rabbit anti-PVF-1 antibody, then for 3 hours each with Texas Red-conjugated goat anti-rabbit secondary antibody (diluted 1:200, Invitrogen) followed by fluorescein-conjugated mouse anti-GFP antibody (diluted 1:100, Creative Diagnostics). A solution of 1× PBS with 1% BSA, 0.5% Triton X-100, 0.05% sodium azide and 1 mM EDTA was used for antibody dilution, while washings used 1× PBS with 0.1% BSA, 0.5% Triton X-100, 0.05% sodium azide and 1 mM EDTA.

Microscopy
Animals were viewed by DIC optics using published procedures (Sulston and Horvitz, 1977). All strains carried *him-5(e1490)* to increase the frequency of males. Some strains carried the *ajm-1::GFP* translational reporter (Simske and Hardin, 2001) visualised using a Leica DMRXA microscope to assess epidermal cell morphologies. Confocal fluorescence images were collected using a Leica DMFLS laser confocal microscope, then analysed using Volocity (Quorum Technologies) or ImageJ software (NCBI). Ray 1 severe displacements were scored. Rays are normally embedded in a cuticular fan at the end of the tail, but are anterior to this fan in animals with severe displacements (see Fig. 1A,B).

Molecular biology
Standard molecular biology methods (Sambrook, 1989) were used unless otherwise noted. Plasmids designated *pPD* were kindly provided by A. Fire (Carnegie Institute, Baltimore, MD, USA).

Isolation of *pvf-1* deletion mutant
The *pvf-1* deletion allele (Fig. 2A) was identified from a reverse genetics library of frozen F2 grand-progeny of EMS-mutagenised Fo animals as described previously (Roy et al., 2000).

Transgene constructs
The previously described *unc-40p::unc40::gfp* transgene array used for rescue studies was obtained by transgenesis with plasmid *pZH22* (Chan et al., 1996). The following constructs were newly designed and cloned in our laboratory (see Fig. 2B): (1) *pvf-1p::cfp* construct (also known as *CFP82*) – a 1900 bp PCR product *Bam*H1 fragment comprising the *pvf-1* promoter cloned into

Fig. 2. The nature of the *pvf-1(ev763)* mutation and constructs used to probe PVF-1 function. (**A**) The organisation of the *pvf-1* locus, including coding (black rectangles) and non-coding regions (adjoining lines). The extent of the *pvf-1(ev763)* deletion is indicated in red. (**B**) Coding and non-coding sequences of the constructs used to probe *pvf-1* function (see Materials and methods) are shown as in A.

plasmid *pPD133.82* (previously deleted for the *myo-3* promoter) upstream of *cfp* and 734 bp of *unc-54* 3′UTR sequence; (2) *pvf-1p::pvf-(+)* construct (also known as PVL95) – a *pvf-1* genomic fragment of 4.9 kb comprising 1.9 kb of the 5′UTR and the entire 2.86 kb of coding sequence with introns plus 390 bp of 3′UTR PCR amplified and cloned into a *Bam*H1-*Apa*I cut *pPD95.75* vector; (3) *myo-3p::pvf-1* construct (also known as PVL97) – the 2.86 kb coding sequence with introns plus 390 bp of 3′UTR of *pvp-1(+)* present in PVL95 (see above) PCR amplified and cloned into *Not*I-*Apa*I cut *pPD133.97* (downstream of the 2.4 kb *myo-3* promoter); (4) *hsp16.41p::pvf-1* construct (also known as PVL83) – the 2.86 kb coding sequence with introns plus 390 bp of 3′UTR of *pvp-1* present in PVL95 (see above) PCR amplified and cloned into *Bam*HI-*Apa*I cut *pPD49.83* (downstream of the *hsp16.41* promoter); (5) *myo-3p::mVEGF164* construct (also known as pZH234) – the 573 bp mouse *VEGF164* cDNA (gift from Dr A. Nagy, University of Toronto, Toronto, Canada) cloned downstream of the 2.4-kb *myo-3* promoter and upstream of the *unc-54* 3′UTR in *Kpn*I-*Sac*I cut *pPD96.52* vector; (6) *ram-5p::ced-10(G12V)* construct – a PCR fusion product of the entire *ced-10(G12V)* cDNA (Lundquist et al., 2001) (a gift from Dr E. Lundquist, University of Kansas, Kansas, USA), the 3221 bp *ram-5* promotor (Yu et al., 2000) and the 723-bp *unc-54* 3′UTR injected; (7) *lin-32p::ver-1* construct (also known as pZH260) – sequenced 3.3 kb *lin-32* promoter (Portman and Emmons, 2000) and the entire 3198 bp *C. elegans ver-1* cDNA cloned in tandem upstream of 735 bp of the *unc-54* 3′UTR in *Hin*DIII-*Nco*I cut *pPD96.52* vector; (8) *lin-32p::hKDR* construct (also known as pZH262) – the entire 4092 bp human *KDR* cDNA (gift of Dr Sandro de Falco, Institute of Genetics and Biophysics, CNR, Naples, Italy) cloned downstream of the *C. elegans lin-32* promoter (Portman and Emmons, 2000) by replacing the *ver-1* gene of pZH260 with the *hKDR* gene; (9) *lin-32p::hFLT* construct (also known as pZH265) – the entire 4017 bp human *FLT* cDNA (a gift from Dr Sandro de Falco) cloned downstream of the 3.3 kb *lin-32* promoter (Portman and Emmons, 2000) and upstream of the 1293 bp human *FLT* 3′UTR.

Germline transformation
Transgenic strains were generated by microinjection of a DNA mix into the distal gonad arms of N2 or *him-5(e1490)* hermaphrodites (Mello and Fire, 1995). DNA mixes consisted of a test construct at a concentration of 50 mg/ml or 30 mg/ml and a co-injection reporter *sur-5::gfp* (Portman and Emmons, 2000) or *myo-3p::yfp* to create a final DNA concentration of 100 mg/ml.

Transgene arrays
The following transgene arrays were established in *him-5(e1490)* hermaphrodites: (1) *evEx442 [pvf-1p::cfp; myo-3p::yfp]*; (2) *evEx429[pvf-1p::pvf-1(+)]*; (3) *evEx430[myo-3p::pvf-1(+)]*; (4) *evEx432[hsp16.2p::pvf-1(+)]* and (5) *evEx431[myo-3p::mVEGF164]*; (6) *evEx433[pvf-1p::pvf-1(+)]*; (7) *evEx434[ram-5p::ced-10(G12V)]*; (8) *evEx437[lin-32p::ver-1]*; (9) *evEx435[lin-32p::hKDR]*; and (10) *evEx436[lin-32p::hFLT]*.

Heat shock
Synchronised strains were grown on NGM plates coated with OP50 bacteria at 20°C until the L2 stage, incubated at 33°C for 2 hours (Stringham et al., 1992), reared at 20°C until the adult stage, then scored for ray 1 displacement defects.

Statistics
Standard errors for percentages of the anterior ray 1 phenotypes were calculated assuming a binomial distribution with the observed percentage value and the actual sample size. Statistical tests were carried out using a standard (two-tailed) comparison of two proportions (Moore, 1998). All *P* values represent the probability that the measured penetrance of the phenotype is significantly different between two strains. A *P<0.05* is considered significant.

RESULTS
PVF-1 expression pattern and genetic characterisation
The *C. elegans pvf-1* gene encodes a small secreted protein (PVF-1) with a VEGF-related sequence that includes the highly conserved
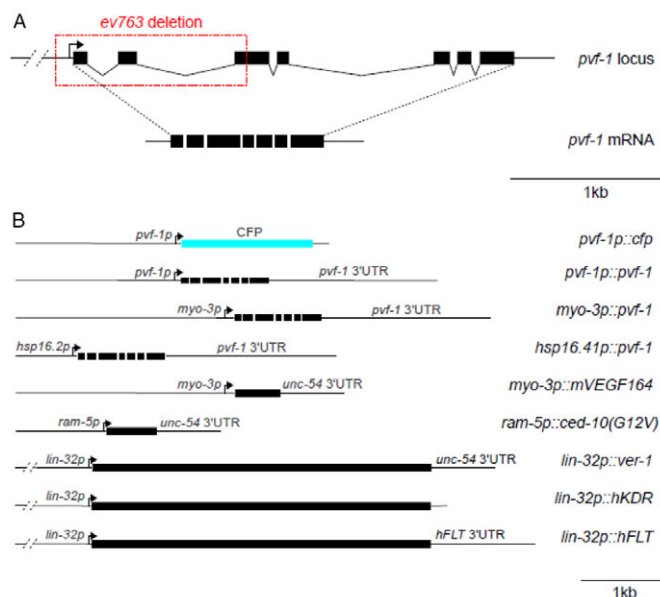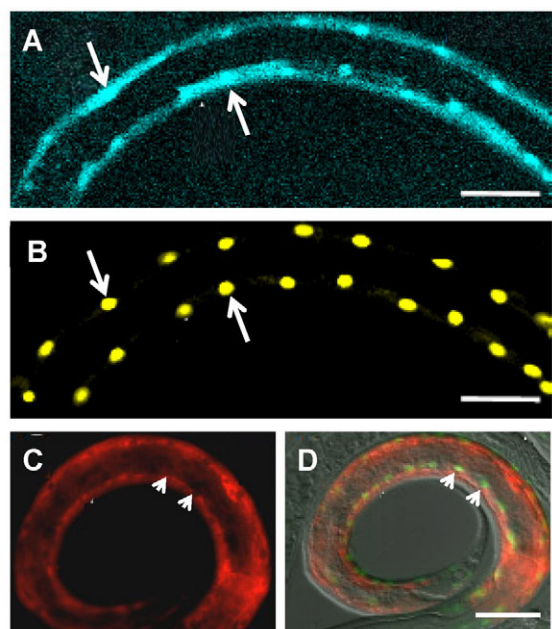
Fig. 3. Epifluorescence and DIC microscopy images of PVF-1 expression in body wall muscles. All views are from a lateral perspective. For the hermaphrodite in A,B, dorsal is upwards and anterior is leftwards. The hermaphrodite in C,D is curled on itself such that the head sits below the tail and, for most of the body, ventral is upwards. (**A,B**) Hermaphrodite carrying an extra-chromosomal array containing *pvf-1p::cfp* and *myo-3p::yfp* transcriptional reporters are shown. There is overlap between CFP-positive dorsal and ventral muscle bands in A (white arrows) and the YFP-positive muscle nuclear reporter in the same animal in B (white arrows). (**C,D**) The immunohistochemical localisation pattern of PVF-1 is shown in hermaphrodites carrying an extrachromosomal array made by co-transformation with *pvf-1p::pvf-1(+)* (rescuing construct *PVL95*) and *myo-3p::yfp* (construct *pPD133.97*) DNAs. (C) A rabbit antibody raised against CePVF-1 (Tarsitano et al., 2006) binds the body wall muscles (Texas Red signal, white arrows). (D) The same animal shows (by DIC of merge for red and green fluorescence) PVF-1 immunofluorescence (red signal, white arrows), and body wall muscle nuclear expression (green signal, white arrows). Scale bars: 38 μm for A,B; in D, 50 μm for C,D.

positioning of cysteines characteristic of the VEGF/PDGF growth factor family (Tarsitano et al., 2006). *C. elegans* PVF-1 has been found to bind human receptors VEGFR1 (FLT1) and VEGFR2 (KDR), and can induce angiogenesis in chick embryos and capillary tube formation in human umbilical vein endothelial cell (HUVEC) culture (Tarsitano et al., 2006).

To study the function of PVF-1 in *C. elegans*, we first examined its expression pattern. The *pvf-1* gene comprises 7 exons and a functionally-sufficient 5′UTR/promoter of 1900 nucleotides (see below). We found that a *pvf-1p::cfp* transcriptional reporter (Fig. 2) drives expression of cyan fluorescence protein (CFP) in dorsal and ventral body wall muscle bands (Fig. 3A), beginning in the first larval (L1) stage, peaking at the L3 stage and slowly diminishing in the adult. The *pvf-1p::cfp* fluorescence colocalises with the yellow fluorescence from a muscle specific *myo-3p::yfp* reporter gene (Fig. 3B). These results are supported by immunofluorescence data (Fig. 3C,D).

To determine the role of *pvf-1* in the development of *C. elegans*, we isolated a *pvf-1* deletion allele (*ev763*) from a reverse genetics library (Zwaal et al., 1993; Roy et al., 2000). This allele contains a 1465 bp deletion that spans a region beginning 405 bp upstream of

the initiation codon and ending after the first 19 bp of exon 3 (Fig. 2A), predicting deletion of the N-terminal 74 (of 304) amino acid residues and absence of an in-frame AUG codon for another 16 residues. Hermaphrodites homozygous for *pvf-1(ev763)* exhibit no obvious developmental or morphological defects. Furthermore, no DA or DB motor axon, touch cell axon, or distal tip cell migration defects were observed using *unc-129::gfp* (MacNeil et al., 2009), *mec-7::gfp* (Hamelin et al., 1992) and *lag-2::gfp* (Blelloch et al., 1999), respectively, as reporters for these cells.

The *plx-1(ev724)* ray 1 anterior displacement phenotype is enhanced by the *pvf-1(ev763)*

We previously showed that semaphorins, UNC-6 and their receptors prevent the anterior displacement of the most anterior ray sensillum (ray 1) in the male tail of *C. elegans* (Dalpé et al., 2004; Dalpé et al., 2012). That neuropilin, the vertebrate semaphorin 3 receptor, also binds VEGF164 prompted us to investigate whether PVF-1 has a function in ray 1 positioning, even though *C. elegans* does not produce a neuropilin homologue. In these studies, *him-5(e1490)* was used to generate a high frequency of males in all of the mutant strains examined, thus *him-5(e1490)* serves as a 'wild-type' control (Fig. 1A; Figs 4-6, line 1). Homozygous *pvf-1(ev763)* males do not display any visible phenotypes or ray displacements (Fig. 4, line 2); however, we found that it significantly enhances a *plx-1(ev724)/plexin* null mutant for ray 1 severe anterior displacements (i.e. displacements anterior to the cuticular fan in which the rays are normally embedded) (Fig. 1A,B,E; Fig. 4, lines 2-4).

Mouse VEGF164 or muscle-specific or heat shock-induced expression of PVF-1 rescues *pvf-1* mutant ray 1 defects

We investigated the cell autonomy of *pvf-1* function by cell type-specific rescue experiments. We found that a *pvf-1p::pvf-1(+)* transgene array (Materials and methods) largely rescues the enhancement of the *plx-1* mutant ray 1 defects caused by *pvf-1(ev763)* (Fig. 4, lines 4,5), as does expressing *pvf-1(+)* under the control of the muscle-specific *myo-3* promotor (Okkema et al., 1993) (Fig. 4, lines 4,6). In principle, PVF-1 secreted from any source could rescue the *pvf-1(ev763)*-mediated enhancement of *plx-1* mutant ray 1 defects if PVF-1 functions permissively. We examined this hypothesis by driving *pvf-1(+)* expression with the heat shock promoter *hsp16.41p* (Okkema et al., 1993). We found that heat shock induced *hsp16.41p::pvf-1(+)* can rescue the *pvf-1(ev763)*-mediated enhancement of *plx-1(ev724)* ray 1 defects (Fig. 4, lines 4,7,8). These data and other genetic interactions described below suggest that PVF-1 is normally secreted by body wall muscles and acts to position ray 1; however, secretion by several tissues may be sufficient for PVF-1 function, suggesting that this function of PVF-1 is permissive.

It was established previously that PVF-1 can substitute for VEGF in vertebrate angiogenesis (Tarsitano et al., 2006). To determine whether the converse is true, we introduced into the *pvf-1(ev763); plx-1(ev724)* double mutant a transgene array in which the *myo-3* promoter drives body wall muscle expression of mouse VEGF-164. We found this array can rescue the *pvf-1(ev763)*-enhanced ray 1 defects of *plx-1(ev724)* (Fig. 4, lines 3,4,9). These results suggest that mouse VEGF164 can functionally substitute for *C. elegans* PVF-1 to position ray 1.

PVF-1 normally inhibits UNC-6 and UNC-40 signalling

The ability of *pvf-1(ev763)*, which fails to cause ray 1 defects on its own, to enhance *plx-1(ev724)* suggests that PVF-1 is required for a
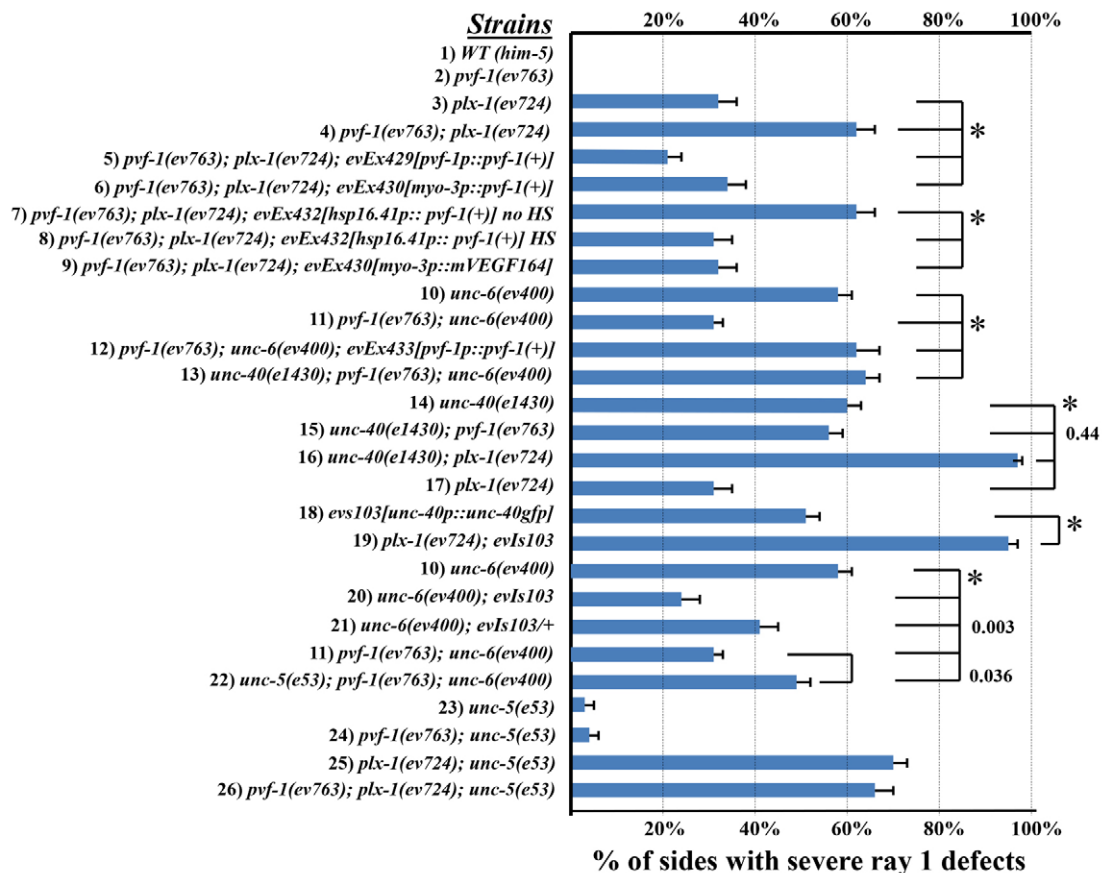
Fig. 4. Genetic interactions between *pvf-1*, *plx-1*, *unc-6*, *unc-40*, *unc-5* and transgene arrays expressing *pvf-1(+)*, *unc-40(+)::gfp* or mouse VEGF164 (*mVEGF164*). The penetrance of ray 1 severe anterior displacement defects (left and right sides of the male tail considered independently) are shown. Corresponding raw data are presented in supplementary material Table S1. All strains carry *him-5(e1490)* mutation, which serves as the wild-type (WT) control. Standard errors for the proportion of animal sides manifesting the ray 1 severe anterior phenotype were calculated assuming a binomial distribution of the same sample size and the observed proportion as mean. Horizontal bars connected by a vertical bar indicate statistical comparisons that were made between the asterisked strain in the group with each of the other strains of the group. The null hypothesis is that the asterisked strain has the same penetrance as each of the strains to which it was compared. All *P* values, except the three shown, were <0.0002.

redundant signal that acts in parallel to PLX-1. We therefore looked for genetic interactions between *pvf-1(ev763)* and mutations in genes that encode components of the UNC-6 signalling pathway. We expected *pvf-1(ev763)* to fail to enhance or suppress *unc-6(ev400)* if PVF-1 is required solely in the UNC-6 pathway for ray 1 positioning. However, we found instead that the penetrance of ray 1 severe displacements in *unc-6(ev400)* males was significantly suppressed by *pvf-1(ev763)*, and that this suppression was reversed by *pvf-1(+)* driven by the 1900 nucleotide *pvf-1* 5′ UTR/promoter (Fig. 4, lines 10-12). Suppression in this case suggests that *pvf-1(ev763)* causes an effective gain of function in some mechanism required for normal ray 1 positioning that compensates for the *unc-6* mutant deficit. As we know of only two signalling mechanisms involved in preventing this ray 1 phenotype (UNC-6/UNC-40 and SMP-1/PLX-1), and we have found that PVF-1 functions in parallel with PLX-1 to prevent ray 1 displacement, it is likely that *pvf-1(ev763)* causes an effective gain of function downstream of UNC-6 in the UNC-6/UNC-40 signal transduction mechanism involved in ray 1 positioning. Consistent with this idea, *pvf-1(ev763)* did not significantly enhance or suppress *unc-40(e1430)*, a predicted null mutant (Chan et al., 1996) for ray 1 defects (Fig. 4, lines 14,15), suggesting that PVF-1 functions in the same pathway as UNC-40. Furthermore, *pvf-1(ev763)* suppression of the *unc-6(ev400)* defects

was largely reverted by *unc-40(ev1430)* (Fig. 4, lines 11,13) to about the same penetrance as *unc-6(ev400)* (Fig. 4, line 10) and the *unc-40(e1430); unc-5(e53); unc-6(ev400)* triple (see Dalpé et al., 2012), as expected if the putative gain of function is downstream of UNC-6 and depends on UNC-40. We conclude that *pvf-1(ev763)* is likely to cause an effective gain of function in UNC-40 or an UNC-40-dependent effector – a gain of function that can enhance a *plx-1* deficit for ray 1 defects, yet can bypass the need for UNC-6 function in this permissive context. As the suppression requires the presence of UNC-40, these data suggest that PVF-1 normally inhibits rather than promotes UNC-6/UNC-40 signalling to prevent the ray 1 displacement. No obvious visible effects on the levels of an *unc-40::gfp* translational reporter were observed (G.D., unpublished results), but these observations do not rule out regulation of UNC-40 levels by PVF-1.

The seemingly contradictory ability of *pvf-1(ev673)* to mimic both an *unc-40* loss of function in one context (e.g. enhancement of the *plx-1* mutant ray 1 defects, see Fig. 4, lines 2-4,14,16) and an effective *unc-40* gain of function in another context (suppression of the *unc-6* mutant ray 1 defects, see Fig. 4, lines 10,11) can be reconciled by data showing that *unc-40(+)* multicopy arrays such as *evIs103* (Fig. 4, line 18) also enhance *plx-1(ev724)* (Fig. 4, lines 17,19) and suppress *unc-6(ev400)* (Fig. 4, lines 10,20,21) (for more

details see Dalpé et al., 2012). Furthermore, as reported in Dalpé et al. (Dalpé et al., 2012), reducing the *unc-40(+)* gene dose of the *evIs103* array from two to one nearly eliminates its ability to cause ray 1 defects (reduced from 45% to 7% penetrance) (Dalpé et al., 2012), while retaining some ability to suppress *unc-6(ev400)* (Fig. 4, lines 10,21). Thus, a predicted high level of UNC-40 activity produced by the *evIs103* array appears capable of interfering with normal ray 1 positioning [probably by interfering with UNC-6-UNC-40 signal transduction as *evIs103* enhances *plx-1(ev724)*], whereas a predicted lower level of UNC-40 overactivity [as when *unc-40(+)* multi-copy array dose is halved or when UNC-6 is non-functional] not only largely fails to interfere with normal ray 1 positioning [except in *plx-1(ev724)*], but also bypasses the need for UNC-6 function.

The finding that *pvf-1(ev763)* largely mimics the effect of a single dose of the *evIs103 unc-40(+)* multicopy array, in that it causes few if any ray 1 defects but suppresses *unc-6 (ev400)* defects, suggests that *pvf-1(ev763)* causes a level of UNC-40 overactivity approximately equivalent to that caused by a single dose of the *evIs103* array (see Dalpé et al., 2012). The suppression of *unc-6* mutant ray 1 defects also partially depends on UNC-5 as shown by the finding that the *unc-6(ev400);pvf-1(ev763);unc-5(e53)* triple mutant has a higher penetrance of ray1 defects than the *unc-6(ev400);pvf-1(ev763)* double (Fig. 4, lines 11,22). However, *pvf-1(ev763)* causes no obvious suppression (or enhancement) of the *unc-5(e53)* ray 1 defect (Fig. 4, lines 23,24). This could result from a minor role for UNC-5 in ray 1 positioning because it functions redundantly with PLX-1 (see Dalpé et al., 2012); however, there was no apparent suppression of the *plx-1(ev724) unc-5(e53)* double mutant ray 1 defects by *pvf-1(ev763)* either (Fig. 4, lines 25,26), suggesting that UNC-5, like UNC-40, is a possible target for inhibition by PVF-1 [although there is no precedent for believing enhanced UNC-5 activity can suppress *unc-6(ev400)*, which there is for UNC-40 activity (Dalpé et al., 2012)].

PVF-1 inhibits CED-10-dependent, but not MIG-2-dependent UNC-40 signalling, to prevent anterior displacement of ray 1

We previously identified the Rho/Rac small GTPase homologues MIG-2 and CED-10 as probable mediators of the semaphorin 1/PLX-1 signal transduction cascade involved in positioning ray 1 (Dalpé et al., 2004). As shown previously, *mig-2(mu28)* and *ced-10(n1993)* mutants have virtually no ray 1 defects (Fig. 5, lines 1-3) but can significantly enhance the ray 1 defects of *plx-1(ev724)* mutants (Fig. 5, lines 4-6). This suggests they each affect a signal transduction pathway that functions redundantly (and therefore in parallel) with the PLX-1 pathway to prevent ray 1 defects, the prime candidate being the UNC-6/UNC-40 pathway (Dalpé et al., 2012). We have also found that *pvf-1(ev763)*, which alone does not cause ray 1 defects and does not significantly enhance *ced-10(n1993)* (Fig. 5, lines 3,7,8), nevertheless does enhance *mig-2(mu28)*, causing synthetic ray 1 anterior displacements in about half of the double mutant animals (Fig. 5, lines 2,7,9). Furthermore, we showed previously that the severe hypomorph *unc-73(rh40)* induced 84% ray 1 severe anterior defects, suggesting that UNC-73/Rho family GEF functions to a large extent in both PLX-1 and UNC-40 signalling in this context. Considered together, the above results are consistent with a model in which (1) MIG-2 and CED-10 function redundantly with one another and with PLX-1, (2) both largely require UNC-73/GEF for their function, and (3) PVF-1 inhibits CED-10-dependent but not MIG-2-dependent UNC-40 signalling to prevent ray 1 displacement in certain genetic contexts (such as a *plx-1* mutant).
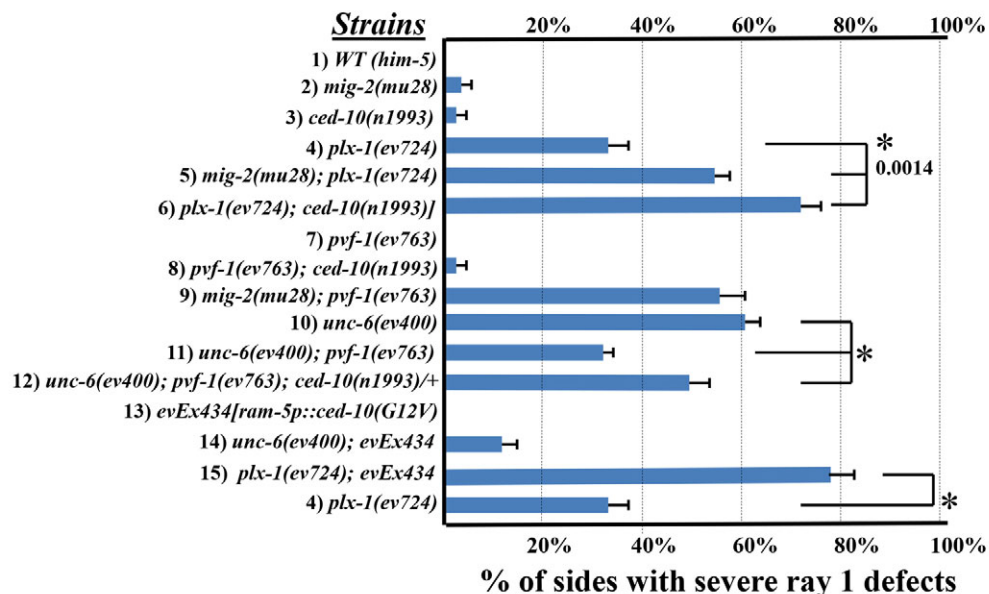

Fig. 5. Genetic interactions between *unc-6*, *pvf-1*, *plx-1*, *ced-10*, *mig-2*, *unc-73* and transgene arrays expressing a *ced-10* gain of function [*ced-10(G12V)*]. All strains carry the *him-5(e1490)* mutation, which serves as the wild-type control. Corresponding raw data are presented in supplementary material Table S2. The frequencies and standard errors for severe (solid bar) anterior ray 1 displacements (left and right sides of the male tail considered independently) are shown for a variety of mutant strains. Standard errors for the proportion of animal sides manifesting the ray 1 severe anterior phenotype were calculated assuming a binomial distribution of the same sample size and the observed proportion as mean. Horizontal bars connected by a vertical bar indicate statistical comparisons that were made between the asterisked strain in the group with each of the other strains of the group. The null hypothesis is that the asterisked strain has the same penetrance as each of the strains to which it was compared. All *P* values, except the three shown, were <0.0002.

A CED-10 gain of function suppresses *unc-6* mutant ray 1 defects

The finding that *pvf-1(ev763)* enhances a *mig-2* deficit but not a *ced-10* deficit raises the possibility that the effective gain of function in UNC-40 activity caused by *pvf-1(ev763)* requires CED-10 but not MIG-2 to induce ray 1 defects. The suppression of *unc-6(ev400)* ray 1 defects by *pvf-1(ev763)* does at least partially depend on CED-10, as shown by the relatively higher penetrance of ray 1 defects in the *unc-6(ev400);pvf-1(ev763);ced-10(n1993)/+* triple mutant compared with the *unc-6(ev400);pvf-1(ev763)* double (Fig. 5, lines 11,12). We could not test the *unc-6(ev400);pvf-1(ev763);ced-10(n1993)* triple mutant because it is lethal; however, an extra-chromosomal transgene array [*evEx434[ram-5p::ced-10(G12V)]*] carrying a gain-of-function mutant *ced-10* cDNA driven by a *ram-5* ray structural cell-specific promoter (Yu et al., 2000) does not display any ray 1 anterior displacement defects in a control *him-5(e1490)* genetic background, but does enhance *plx-1(ev724)* (Fig. 5, lines 4,13,15) and largely rescues *unc-6(ev400)* 1 defects (Fig. 5, lines 10,14) somewhat better than does the *evIs103[unc-40(+)]* multi-copy array (Fig. 4, lines 10,18,20,21). These results suggest that CED-10 normally functions downstream of UNC-40 in the ray 1 structural cell to transduce a permissive signal from UNC-6 to UNC-40 required to prevent the anterior displacement of ray 1, and that a CED-10 gain of function can bypass the need for UNC-6 signalling, at least as well as *pvf-1(ev763)* or an *unc-40(+)* multi-copy array can. These rescue results support a permissive role for UNC-6 in ray 1 positioning and identify CED-10 and not MIG-2 as a target of enhanced UNC-40 activity caused by *pvf-1(ev763)* (see also Dalpé et al., 2012).

C. elegans VERs (VEGF-related receptors) and vertebrate FLT and KDR VEGF receptors function in the PVF-1 signalling pathway for ray 1 positioning

Because the vertebrate VEGF receptors are able to mediate VEGF-like signalling by PVF-1 in vertebrates (Tarsitano et al., 2006), we wondered whether putative vascular endothelial growth factor receptors (VERs) of *C. elegans* could also mediate PVF-1 signalling to position ray 1 in *C. elegans* males. Four *ver* genes that encode a family of four RTKs structurally related to VEGF receptors (VEGFRs) were identified previously (Popovici et al., 2002) and reported to express in specialised cells of neural origin such as glial support cells of amphid and phasmid neurons (VER-1), in the chemosensory ADL neurons (VER-2), and in the ALA neurons (VER-3) of *C. elegans* (Popovici et al., 2002). None of the putative null deletion alleles: *ver-1(ok1738)*, *ver-2(ok897)*, *ver-3(gk227)* or *ver-4(ok1079)* (supplementary material Fig. S1) caused a significant male phenotype (Fig. 6, lines 1-5); however, each *ver* mutation significantly enhanced *plx-1(ev724)* defects to roughly the same extent that *pvf-1(ev763)* did (Fig. 6, lines 6-12). Furthermore, *ver-1*, *ver-2* and *ver-4* mutations each suppressed *unc-6(ev400)* ray 1 defects to approximately the same extent as did *pvf-1(ev763)* (Fig. 6, lines 13-17). We could not test *ver-3(gk227)* for this phenotype because the *unc-6(ev400) ver-3(gk227)* double mutant is lethal.

The similar penetrance of the *ver* mutant defects in two functional assays for ray 1 positioning [enhancement of *plx-1(ev724)* and suppression of *unc-6(ev400)*] raises the possibility that the VERs function interdependently (possibly as a higher-order heteromultimer, see Discussion) and in the same signalling pathway
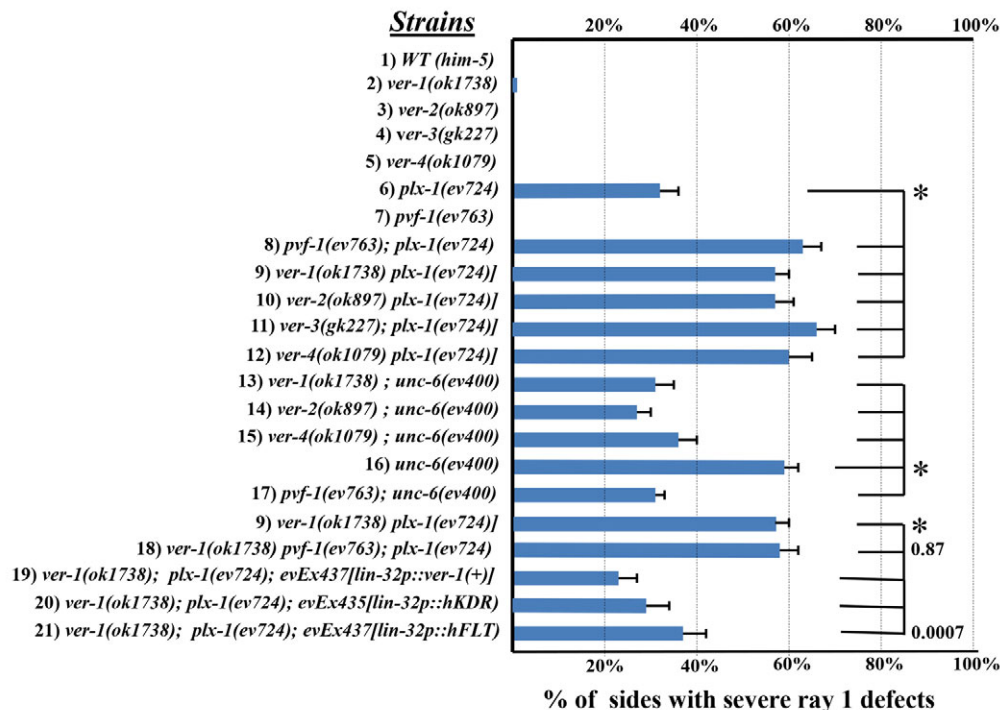

Fig. 6. Genetic interactions between *pvf-1*, *ver-1*, *ver-2*, *ver-3*, *ver-4*, *plx-1*, *unc-6* and transgene arrays expressing VER-1 or human VEGF receptors (hKDR and hFLT). All strains carry the *him-5(e1490)* mutation, which serves as the wild-type control. The frequencies and standard errors for severe (solid bar) anterior ray 1 displacements (left and right sides of the male tail considered independently) are shown for a variety of mutant strains. Corresponding raw data are presented in supplementary material Table S3. Standard errors for the proportion of animal sides manifesting the ray 1 severe anterior phenotype were calculated assuming a binomial distribution of the same sample size and the observed proportion as mean. Horizontal bars connected by a vertical bar indicate statistical comparisons that were made between the asterisked strain in the group with each of the other strains of the group. The null hypothesis is that the asterisked strain has the same penetrance as each of the strains to which it was compared. All *P* values, except the three shown, were <0.0002.

as PVF-1 to position ray 1. To examine the latter possibility, we made a *ver-1(ok1738) pvf-1(ev763); plx-1(ev724)* triple mutant and found *ver-1* and *pvf-1* mutations together enhance the *plx-1* mutant defects to the same extent as the individual *ver-1* and *pvf-1* mutations (Fig. 6, lines 6-9,18). We conclude that VER-1 functions in the same pathway as PVF-1 to prevent ray 1 defects.

UNC-40 and PLX-1 function in the ray support cell to position ray 1, as determined by rescue of the ray 1 defect using the *ram-5* 5′UTR/promoter (Yu et al., 2000) to drive expression of *unc-40(+)* and *plx-1(+)* (Dalpé et al., 2012). We have now found that the *ver-1(ok1738); plx-1(ev724)* double mutant was rescued for the *ver-1* mutant enhancement of *plx-1(ev724)* ray 1 defects by *lin-32* promoter-driven *ver-1(+)* when compared with controls (Fig. 6, lines 2,6,9,18,19), suggesting that VER-1 could function in the same cells as UNC-40 and PLX-1 for ray 1 positioning. This is supported by the support cell focus of CED-10(G12V) activity reported above.

As PVF-1 can bind human VEGFR1 (FLT) and VEGFR2 (KDR) (Tarsitano et al., 2006), we wondered whether human FLT and KDR cDNAs could substitute for CeVER-1 in rescue of the ray 1 defect. We found that *plx-1(ev724);ver-1(ok1738)* double mutant animals carrying *lin-32p::hKDR* (Fig. 6, lines 18,20) or *lin-32p::hFLT* (Fig. 6, lines 18,21) transgene arrays can rescue to nearly the same extent as the *lin-32p::ver-1(+)* array (Fig. 6, lines 18,19). These results demonstrate an evolutionary conservation of VEGF signalling core components in positioning ectodermally derived cells in an animal devoid of a cardiovascular system.

DISCUSSION

The VEGF/PDGF growth factors function in cardiovascular development across many vertebrate species, including humans. These factors induce endothelial cell differentiation and guide their migrations as they undergo morphological changes to form blood vessels (Rousseau et al., 2000; Poole et al., 2001; Zachary et al., 2005; Lamalice et al., 2006; Koch and Claesson-Welsh, 2012). Their functions outside angiogenesis are not as well characterised; however, *Drosophila* PVF-1 has a role in border cell migration in *Drosophila* ovaries (McDonald et al., 2003; Mackenzie and Ruhrberg, 2012) and VEGF can act as a guidance cue by attracting commissural axons to the floor plate of the spinal cord (Ruiz de Almodovar et al., 2011) and by guiding migration of nerve cell soma (Schwarz et al., 2004). *C. elegans* PVF-1 is a secreted protein able to bind human VEGFR1 and VEGFR2, and induce vascular development in chick embryos and capillary tube formation in HUVEC cultures (Tarsitano et al., 2006). *C. elegans* PVF-1 therefore appears to be an excellent candidate VEGF homologue whose developmental role is still undefined, but could act in ways that mirror VEGF roles in vertebrates.

In this paper, we report that a *C. elegans pvf-1* deletion allele does not manifest any obvious phenotype, but enhances the ray 1 anterior displacement phenotype of *plx-1(ev724)*, suggesting that PVF-1 acts redundantly with PLX-1 to position ray 1. We recently identified UNC-6 signalling through UNC-40 and UNC-5 receptors as the predominant signalling mechanism that functions in parallel with PLX-1 to prevent anterior displacement of ray 1 (Dalpé et al., 2012), thus PVF-1 likely regulates UNC-40 and UNC-5 signalling in this context. Here, we present strong evidence that PVF-1 (acting through VER-1 and possibly other VEGF receptors or VERs) normally inhibits UNC-6 signalling through UNC-40 (and UNC-5) and the Rho family GTPase CED-10, but not MIG-2. The logic leading to this conclusion is complicated by the finding that in some multiple mutant combinations *pvf-1(ev763)* mimics an *unc-40* loss-of-function mutation [i.e. it enhances a *plx-1(ev724)*] and in others

it mimics a predicted *unc-40* gain of function [(gf)] [i.e. it suppresses *unc-6(ev400)*]. These apparently opposite effects of *pvf-1(ev763)* are mimicked by a multi-copy *unc-40(+)* array, ev*Is103*, which is predicted to cause UNC-40 overactivity. We reported previously that two doses of this array causes significant ray 1 defects, whereas one dose causes many fewer defects yet still significantly enhances *plx-1(ev724)* (Dalpé et al., 2012). Here, we show that one dose of this array is sufficient to suppress *unc-6(ev400)* defects almost as well as *pvf-1(ev763)* does. Thus, all of the effects of *pvf-1(ev763)* on ray 1 positioning, including its inability to enhance *plx-1* mutant defects and suppress *unc-6* mutant ray 1 defects can be mimicked by a multi-copy *unc-40(+)* array and predicted accompanying UNC-40 over-activity. This leads to the suggestion that *pvf-1(ev763)* causes an effective UNC-40 gain of function roughly equivalent to that caused by a single dose of the multi-copy *unc-40(+)* array.

We hypothesised previously that the *evIs103[unc-40(+)]* multi-copy array creates a partially UNC-6 dependent UNC-40 over-activity that interferes with UNC-6-UNC-40 signal transduction – an activity that is reduced below some threshold for interference by eliminating the activation of UNC-40 by UNC-6 (or by halving the dose of *evIs103*), while retaining enough UNC-40 overactivity to partially bypass the need for UNC-6. *pvf-1(ev763)* is predicted to cause some UNC-40-interfering overactivation of UNC-40 signal transduction in this context – enough to enhance a *plx-1* mutant, but not enough to cause a ray 1 defect on its own. Substantial support for this hypothesis is provided by the finding that the ability of *pvf-1(ev763)* to rescue *unc-6(ev400)* for ray 1 defects depends on UNC-40 activity.

Double mutant analyses demonstrate that, like PVF-1, UNC-5 and CED-10 function redundantly with PLX-1 and in the same pathway with one another. The *ced-10(gf)* array mimics *pvf-1(ev763)* in its abilities to enhance *plx-1(ev724)* and to suppress *unc-6(ev400)* for ray 1 defects, suggesting that CED-10 acts downstream of UNC-6 and by inference UNC-40 in this context. The finding that *unc-40(e1430)*, a putative null allele (Chan et al., 1996), causes significantly more penetrant ray 1 defects than *unc-5(e53)*, suggests that UNC-40 function in ray 1 positioning is at least partially UNC-5 independent. Moreover, the ability of *unc-5(e53)* to revert the suppression of *unc-6(ev400)* by *pvf-1(ev763)*, but less so than the putative *unc-40(e1430)* null allele (Chan et al., 1996), suggests that UNC-5 activity or UNC-40-dependent UNC-5 activity is also regulated by PVF-1 in the same way but possibly not to the same extent that UNC-5-independent UNC-40 activity is.

Taken together, the above results suggest the following molecular model for the way PLX-1, UNC-40 and PVF-1 function to prevent the anterior displacement of ray 1 (Fig. 7). PVF-1 is made and secreted by body wall muscles and binds to one or more VER receptors on the ray 1 glia-like structural cell. The VER receptors transduce a signal to the UNC-40 signalling pathway (possibly including some UNC-5-dependent UNC-40 signalling) that inhibits CED-10 (known to mediate UNC-40 axon guidance signalling) (see Gitai et al., 2003), possibly at the level of UNC-40 or CED-10 GTPase function, but not MIG-2-dependent UNC-40 signalling. This inhibition helps set a level of UNC-6 signalling that is necessary for proper ray 1 positioning in certain genetic contexts (e.g. in a *plx-1* mutant), but not in the wild-type laboratory strain. It remains to be determined therefore what selective pressures caused the evolution of the inhibitory interaction between PVF-1 and UNC-40 signalling revealed here.

While these studies were in progress, it was reported that *ver-1* deletions prevent the dauer-induced structural remodelling of the anterior tip of the glia-like amphid socket cell (Procko et al., 2011),
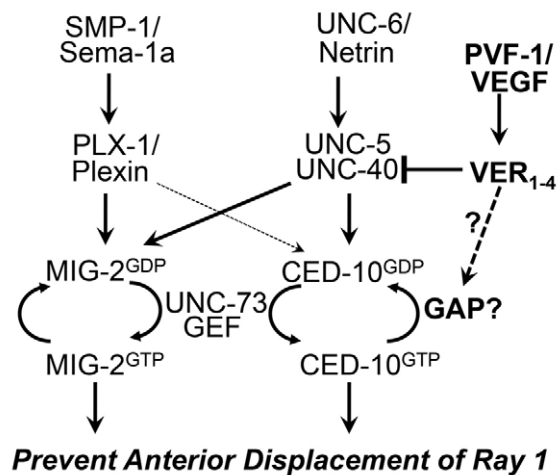
Fig. 7. Model for the role of PVF-1 during ray1 positioning. PVF-1 expressed from body wall muscles functions permissively in a pathway parallel to SMP-1 and PLX-1 for ray1 positioning. MIG-2 functions somewhat in both pathways, whereas CED-10 functions largely in the UNC-6/UNC-40 pathway and may (thin arrow) also function in the PLX-1 pathway (Dalpé et al., 2004). PVF-1 functions in the UNC-6 signalling pathway, which comprises UNC-40, UNC-5 and CED-10. PVF-1 inhibits signalling through the UNC-5- and CED-10-dependent, MIG-2-independent, UNC-40 signalling pathway and an UNC-5-independent UNC-40 signalling pathway. This inhibition is revealed by the ability of *pvf-1* mutants to suppress *unc-6* mutant anterior ray1 defects. Animals carrying evIs103[unc-40p::unc-40::gfp] or evEx434[ram-5p::ced-10(G12V)] gain-of-function transgene arrays phenocopy the *pvf-1* loss-of-function mutants in their ability to suppress the *unc-6* mutant defects. There is a possibility that PVF-1 normally inhibits CED-10 GTPase activity in this context by activating a CED-10-specific GTPase-activating protein (GAP) (dashed arrow and question mark).

which encircles the sensory endings of the amphid sensory neurons (Perkins et al., 1986), just as the ray structural cells are glia-like cells that encircle the sensory endings of the ray neurons. As the ray 1 structural cell is most intimately involved in determining the position of ray 1 (Dalpé et al., 2012) and seems to be the focus of CED-10 (see *ced-10* gain-of-function results), PLX-1 and UNC-40 activity in this process, it raises the possibility that *ver-1* and possibly *pvf-1* and the other *ver* genes function in glia-like structural cell shape changes that accompany dauer formation, as well as positioning ray 1 in the male tail.

It is somewhat surprising that, in combination with *plx-1(ev724)*, the *ver* mutations each cause roughly the same penetrance of ray 1 defects as *pvf-1(ev763)*. This finding does not readily fit with the known function of mammalian VEGF receptors as homodimers and heterodimers (Huang et al., 2001; Nilsson et al., 2010). Our observations suggest that either the *pvf-1* mutation is not null, or there is PVF-1-independent VER function in the context of ray 1 positioning, or the VER receptor comprises a higher order multimer, requiring all four VER subunits for function. Further study of the *ver* genes should help distinguish between these possibilities.

The ability of mammalian VEGF and VEGF receptors to rescue corresponding mutants of *C. elegans* in the context of ray 1 positioning demonstrates that the molecular function of these proteins is conserved from worms to humans. Although the overall logic of ray 1 positioning in *C. elegans* and wiring of the vertebrate vascular system are clearly different, steps in these processes could be mechanistically related. The place to look for relevance of our

findings would be netrin-mediated angiogenic functions involving DCC, the vertebrate homologue of UNC-40 (Keino-Masu et al., 1996). Most data regarding netrin function in angiogenesis show that UNC-5B (and not DCC) activation by netrin 1 regulates angiogenesis by preventing filopodial extension of endothelial cells to limit branching morphogenesis (Suchting et al., 2006), whereas there are limited data suggesting that DCC is expressed by endothelial cells (Nguyen and Cai, 2006) and only correlative evidence that netrin 4 might function through DCC to enhance angiogenesis in a mouse cerebral ischemia model (Hoang et al., 2009). However, there is reasonable evidence that netrin 4, which has anti-angiogenic properties, could function in this context by binding the DCC paralogue neogenin, which then recruits UNC-5B (Wilson et al., 2006; Qin et al., 2007; Lejmi et al., 2008). As our results leave open the possibility that UNC-5-dependent UNC-40 signalling is negatively regulated by VEGF signalling, it is possible that the proposed anti-angiogenic effects of netrin 4 signalling could be regulated by VEGF.

Competing interests statement
The authors declare no competing financial interests.

Author contributions
G.D. performed all of the genetic experiments reported in this manuscript. M.T. and G.P. began this project and provided expression data for *pvf-1*. H.Z. made constructs and transgenic animals for this project. J.C. co-wrote the manuscript with G.D.

Supplementary material
Supplementary material available online at
http://dev.biologists.org/lookup/suppl/doi:10.1242/dev.095190/-/DC1

References
Ackerman, S. L., Kozak, L. P., Przyborski, S. A., Rund, L. A., Boyer, B. B. and Knowles, B. B. (1997). The mouse rostral cerebellar malformation gene encodes an UNC-5-like protein. *Nature* **386**, 838-842.

Bettinger, J. C., Lee, K. and Rougvie, A. E. (1996). Stage-specific accumulation of the terminal differentiation factor LIN-29 during Caenorhabditis elegans development. *Development* **122**, 2517-2527.

Blelloch, R., Anna-Arriola, S. S., Gao, D., Li, Y., Hodgkin, J. and Kimble, J. (1999). The gon-1 gene is required for gonadal morphogenesis in Caenorhabditis elegans. *Dev. Biol.* **216**, 382-393.

Bouvrée, K., Larrivée, B., Lv, X., Yuan, L., DeLafarge, B., Freitas, C., Mathivet, T., Bréant, C., Tessier-Lavigne, M., Bikfalvi, A. et al. (2008). Netrin-1 inhibits sprouting angiogenesis in developing avian embryos. *Dev. Biol.* **318**, 172-183.

Chan, S. S., Zheng, H., Su, M. W., Wilk, R., Killeen, M. T., Hedgecock, E. M. and Culotti, J. G. (1996). UNC-40, a C. elegans homolog of DCC (Deleted in Colorectal Cancer), is required in motile cells responding to UNC-6 netrin cues. *Cell* **87**, 187-195.

Dalpé, G., Zhang, L. W., Zheng, H. and Culotti, J. G. (2004). Conversion of cell movement responses to Semaphorin-1 and Plexin-1 from attraction to repulsion by lowered levels of specific RAC GTPases in C. elegans. *Development* **131**, 2073-2088.

Dalpé, G., Zheng, H., Brown, L. and Culotti, J. G. (2012). Semaphorin-1 and netrin signal in parallel and permissively to position the male ray 1 sensillum in Caenorhabditis elegans. *Genetics* **192**, 959-971.

Ellis, R. E., Jacobson, D. M. and Horvitz, H. R. (1991). Genes required for the engulfment of cell corpses during programmed cell death in Caenorhabditis elegans. *Genetics* **129**, 79-94.

Emmons, S. W. (2005). Male development. In *WormBook* (ed. The C. elegans Research Community), pp. 1-22. doi/10.1895/wormbook.1.33.1.

Gitai, Z., Yu, T. W., Lundquist, E. A., Tessier-Lavigne, M. and Bargmann, C. I. (2003). The netrin receptor UNC-40/DCC stimulates axon attraction and outgrowth through enabled and, in parallel, Rac and UNC-115/AbLIM. *Neuron* **37**, 53-65.

Hamelin, M., Scott, I. M., Way, J. C. and Culotti, J. G. (1992). The mec-7 beta-tubulin gene of Caenorhabditis elegans is expressed primarily in the touch receptor neurons. *EMBO J.* **11**, 2885-2893.

Hedgecock, E. M., Culotti, J. G. and Hall, D. H. (1990). The unc-5, unc-6, and unc-40 genes guide circumferential migrations of pioneer axons and mesodermal cells on the epidermis in C. elegans. *Neuron* **4**, 61-85.

Hinck, L. (2004). The versatile roles of "axon guidance" cues in tissue morphogenesis. *Dev. Cell* **7**, 783-793.

Hoang, S., Liauw, J., Choi, M., Choi, M., Guzman, R. G. and Steinberg, G. K. (2009). Netrin-4 enhances angiogenesis and neurologic outcome after cerebral ischemia. *J. Cereb. Blood Flow Metab.* **29**, 385-397.

Hodgkin, J. A. and Brenner, S. (1977). Mutations causing transformation of sexual phenotype in the nematode Caenorhabditis elegans. *Genetics* **86**, 275-287.

Huang, K., Andersson, C., Roomans, G. M., Ito, N. and Claesson-Welsh, L. (2001). Signaling properties of VEGF receptor-1 and -2 homo- and heterodimers. *Int. J. Biochem. Cell Biol.* **33**, 315-324.

Ishii, N., Wadsworth, W. G., Stern, B. D., Culotti, J. G. and Hedgecock, E. M. (1992). UNC-6, a laminin-related protein, guides cell and pioneer axon migrations in C. elegans. *Neuron* **9**, 873-881.

Keino-Masu, K., Masu, M., Hinck, L., Leonardo, E. D., Chan, S. S., Culotti, J. G. and Tessier-Lavigne, M. (1996). Deleted in Colorectal Cancer (DCC) encodes a netrin receptor. *Cell* **87**, 175-185.

Koch, S. and Claesson-Welsh, L. (2012). Signal transduction by vascular endothelial growth factor receptors. *Cold Spring Harb Perspect Med* **2**, a006502.

Kolodkin, A. L., Matthes, D. J., O'Connor, T. P., Patel, N. H., Admon, A., Bentley, D. and Goodman, C. S. (1992). Fasciclin IV: sequence, expression, and function during growth cone guidance in the grasshopper embryo. *Neuron* **9**, 831-845.

Kolodkin, A. L., Matthes, D. J. and Goodman, C. S. (1993). The semaphorin genes encode a family of transmembrane and secreted growth cone guidance molecules. *Cell* **75**, 1389-1399.

Lai Wing Sun, K., Correia, J. P. and Kennedy, T. E. (2011). Netrins: versatile extracellular cues with diverse functions. *Development* **138**, 2153-2169.

Lamalice, L., Houle, F. and Huot, J. (2006). Phosphorylation of Tyr1214 within VEGFR-2 triggers the recruitment of Nck and activation of Fyn leading to SAPK2/p38 activation and endothelial cell migration in response to VEGF. *J. Biol. Chem.* **281**, 34009-34020.

Larrivée, B., Freitas, C., Trombe, M., Lv, X., Delafarge, B., Yuan, L., Bouvrée, K., Bréant, C., Del Toro, R., Bréchot, N. et al. (2007). Activation of the UNC5B receptor by Netrin-1 inhibits sprouting angiogenesis. *Genes Dev.* **21**, 2433-2447.

Lejmi, E., Leconte, L., Pédron-Mazoyer, S., Ropert, S., Raoul, W., Lavalette, S., Bouras, I., Feron, J. G., Maitre-Boube, M., Assayag, F. et al. (2008). Netrin-4 inhibits angiogenesis via binding to neogenin and recruitment of Unc5B. *Proc. Natl. Acad. Sci. USA* **105**, 12491-12496.

Leonardo, E. D., Hinck, L., Masu, M., Keino-Masu, K., Ackerman, S. L. and Tessier-Lavigne, M. (1997). Vertebrate homologues of C. elegans UNC-5 are candidate netrin receptors. *Nature* **386**, 833-838.

Leung-Hagesteijn, C., Spence, A. M., Stern, B. D., Zhou, Y., Su, M. W., Hedgecock, E. M. and Culotti, J. G. (1992). UNC-5, a transmembrane protein with immunoglobulin and thrombospondin type 1 domains, guides cell and pioneer axon migrations in C. elegans. *Cell* **71**, 289-299.

Lu, X., Le Noble, F., Yuan, L., Jiang, Q., De Lafarge, B., Sugiyama, D., Bréant, C., Claes, F., De Smet, F., Thomas, J. L. et al. (2004). The netrin receptor UNC5B mediates guidance events controlling morphogenesis of the vascular system. *Nature* **432**, 179-186.

Lundquist, E. A., Reddien, P. W., Hartwieg, E., Horvitz, H. R. and Bargmann, C. I. (2001). Three C. elegans Rac proteins and several alternative Rac regulators control axon guidance, cell migration and apoptotic cell phagocytosis. *Development* **128**, 4475-4488.

Luo, Y., Raible, D. and Raper, J. A. (1993). Collapsin: a protein in brain that induces the collapse and paralysis of neuronal growth cones. *Cell* **75**, 217-227.

Mackenzie, F. and Ruhrberg, C. (2012). Diverse roles for VEGF-A in the nervous system. *Development* **139**, 1371-1380.

MacNeil, L., Hardy, W. R., Wrana, J. L. and Culotti, J. G. (2009). The TGF-B family member UNC-129 alters the response to UNC-6/Netrin by regulating the balance between UNC-40 dependent and independent UNC-5 signaling. *Nat. Neurosci.* **12**, 150-155.

McDonald, J. A., Pinheiro, E. M. and Montell, D. J. (2003). PVF1, a PDGF/VEGF homolog, is sufficient to guide border cells and interacts genetically with Taiman. *Development* **130**, 3469-3478.

Mello, C. and Fire, A. (1995). DNA transformation. *Methods Cell Biol.* **48**, 451-482.

Merz, D. C., Zheng, H., Killeen, M. T., Krizus, A. and Culotti, J. G. (2001). Multiple signaling mechanisms of the UNC-6/netrin receptors UNC-5 and UNC-40/DCC in vivo. *Genetics* **158**, 1071-1080.

Moore, D. S. and McCabe, G. P. (1998). *Introduction To The Practice Of Statistics.* New York, NY: WH Freeman.

Nguyen, A. and Cai, H. (2006). Netrin-1 induces angiogenesis via a DCC-dependent ERK1/2-eNOS feed-forward mechanism. *Proc. Natl. Acad. Sci. USA* **103**, 6530-6535.

Nilsson, I., Bahram, F., Li, X., Gualandi, L., Koch, S., Jarvius, M., Söderberg, O., Anisimov, A., Kholová, I., Pytowski, B. et al. (2010). VEGF receptor 2/-3 heterodimers detected in situ by proximity ligation on angiogenic sprouts. *EMBO J.* **29**, 1377-1388.

Okkema, P. G., Harrison, S. W., Plunger, V., Aryana, A. and Fire, A. (1993). Sequence requirements for myosin gene expression and regulation in Caenorhabditis elegans. *Genetics* **135**, 385-404.

Park, K. W., Crouse, D., Lee, M., Karnik, S. K., Sorensen, L. K., Murphy, K. J., Kuo, C. J. and Li, D. Y. (2004). The axonal attractant Netrin-1 is an angiogenic factor. *Proc. Natl. Acad. Sci. USA* **101**, 16210-16215.

Perkins, L. A., Hedgecock, E. M., Thomson, J. N. and Culotti, J. G. (1986). Mutant sensory cilia in the nematode Caenorhabditis elegans. *Dev. Biol.* **117**, 456-487.

Poole, T. J., Finkelstein, E. B. and Cox, C. M. (2001). The role of FGF and VEGF in angioblast induction and migration during vascular development. *Dev. Dyn.* **220**, 1-17.

Popovici, C., Isnardon, D., Birnbaum, D. and Roubin, R. (2002). Caenorhabditis elegans receptors related to mammalian vascular endothelial growth factor receptors are expressed in neural cells. *Neurosci. Lett.* **329**, 116-120.

Portman, D. S. and Emmons, S. W. (2000). The basic helix-loop-helix transcription factors LIN-32 and HLH-2 function together in multiple steps of a C. elegans neuronal sublineage. *Development* **127**, 5415-5426.

Procko, C., Lu, Y. and Shaham, S. (2011). Glia delimit shape changes of sensory neuron receptive endings in C. elegans. *Development* **138**, 1371-1381.

Qin, S., Yu, L., Gao, Y., Zhou, R. and Zhang, C. (2007). Characterization of the receptors for axon guidance factor netrin-4 and identification of the binding domains. *Mol. Cell. Neurosci.* **34**, 243-250.

Rousseau, S., Houle, F. and Huot, J. (2000). Integrating the VEGF signals leading to actin-based motility in vascular endothelial cells. *Trends Cardiovasc. Med.* **10**, 321-327.

Roy, P. J., Zheng, H., Warren, C. E. and Culotti, J. G. (2000). mab-20 encodes Semaphorin-2a and is required to prevent ectopic cell contacts during epidermal morphogenesis in Caenorhabditis elegans. *Development* **127**, 755-767.

Ruiz de Almodovar, C., Fabre, P. J., Knevels, E., Coulon, C., Segura, I., Haddick, P. C., Aerts, L., Delattin, N., Strasser, G., Oh, W. J. et al. (2011). VEGF mediates commissural axon chemoattraction through its receptor Flk1. *Neuron* **70**, 966-978.

Sambrook, J., Fritsch, E. F. and Maniatis, T. (1989). *Molecular Cloning: A Laboratory Manual.* Plainview, NY: Cold Spring Harbor Laboratory Press.

Schwarz, Q., Gu, C., Fujisawa, H., Sabelko, K., Gertsenstein, M., Nagy, A., Taniguchi, M., Kolodkin, A. L., Ginty, D. D., Shima, D. T. et al. (2004). Vascular endothelial growth factor controls neuronal migration and cooperates with Sema3A to pattern distinct compartments of the facial nerve. *Genes Dev.* **18**, 2822-2834.

Serafini, T., Colamarino, S. A., Leonardo, E. D., Wang, H., Beddington, R., Skarnes, W. C. and Tessier-Lavigne, M. (1996). Netrin-1 is required for commissural axon guidance in the developing vertebrate nervous system. *Cell* **87**, 1001-1014.

Simske, J. S. and Hardin, J. (2001). Getting into shape: epidermal morphogenesis in Caenorhabditis elegans embryos. *Bioessays* **23**, 12-23.

Stringham, E. G., Dixon, D. K., Jones, D. and Candido, E. P. (1992). Temporal and spatial expression patterns of the small heat shock (hsp16) genes in transgenic Caenorhabditis elegans. *Mol. Biol. Cell* **3**, 221-233.

Suchting, S., Bicknell, R. and Eichmann, A. (2006). Neuronal clues to vascular guidance. *Exp. Cell Res.* **312**, 668-675.

Sulston, J. E. and Horvitz, H. R. (1977). Post-embryonic cell lineages of the nematode, Caenorhabditis elegans. *Dev. Biol.* **56**, 110-156.

Sulston, J. E., Albertson, D. G. and Thomson, J. N. (1980). The Caenorhabditis elegans male: postembryonic development of nongonadal structures. *Dev. Biol.* **78**, 542-576.

Tarsitano, M., De Falco, S., Colonna, V., McGhee, J. D. and Persico, M. G. (2006). The C. elegans pvf-1 gene encodes a PDGF/VEGF-like factor able to bind mammalian VEGF receptors and to induce angiogenesis. *FASEB J.* **20**, 227-233.

Tessier-Lavigne, M., Placzek, M., Lumsden, A. G., Dodd, J. and Jessell, T. M. (1988). Chemotropic guidance of developing axons in the mammalian central nervous system. *Nature* **336**, 775-778.

Testori, J., Schweighofer, B., Helfrich, I., Sturtzel, C., Lipnik, K., Gesierich, S., Nasarre, P., Hofer-Warbinek, R., Bilban, M., Augustin, H. G. et al. (2011). The VEGF-regulated transcription factor HLX controls the expression of guidance cues and negatively regulates sprouting of endothelial cells. *Blood* **117**, 2735-2744.

Wadsworth, W. G., Bhatt, H. and Hedgecock, E. M. (1996). Neuroglia and pioneer neurons express UNC-6 to provide global and local netrin cues for guiding migrations in C. elegans. *Neuron* **16**, 35-46.

Wilson, B. D., Ii, M., Park, K. W., Suli, A., Sorensen, L. K., Larrieu-Lahargue, F., Urness, L. D., Suh, W., Asai, J., Kock, G. A. et al. (2006). Netrins promote developmental and therapeutic angiogenesis. *Science* **313**, 640-644.

Wood, W. B. (1988). *The Nematode Caenorhabditis elegans*. Cold Spring Harbour, NY: Cold Spring Harbor Laboratory Press.

Yu, R. Y., Nguyen, C. Q., Hall, D. H. and Chow, K. L. (2000). Expression of ram-5 in the structural cell is required for sensory ray morphogenesis in Caenorhabditis elegans male tail. *EMBO J.* **19**, 3542-3555.

Zachary, A. A., Montgomery, R. A. and Leffell, M. S. (2005). Factors associated with and predictive of persistence of donor-specific antibody after treatment with plasmapheresis and intravenous immunoglobulin. *Hum. Immunol.* **66**, 364-370.

Zipkin, I. D., Kindt, R. M. and Kenyon, C. J. (1997). Role of a new Rho family member in cell migration and axon guidance in C. elegans. *Cell* **90**, 883-894.

Zwaal, R. R., Broeks, A., van Meurs, J., Groenen, J. T. and Plasterk, R. H. (1993). Target-selected gene inactivation in Caenorhabditis elegans by using a frozen transposon insertion mutant bank. *Proc. Natl. Acad. Sci. USA* **90**, 7431-7435.
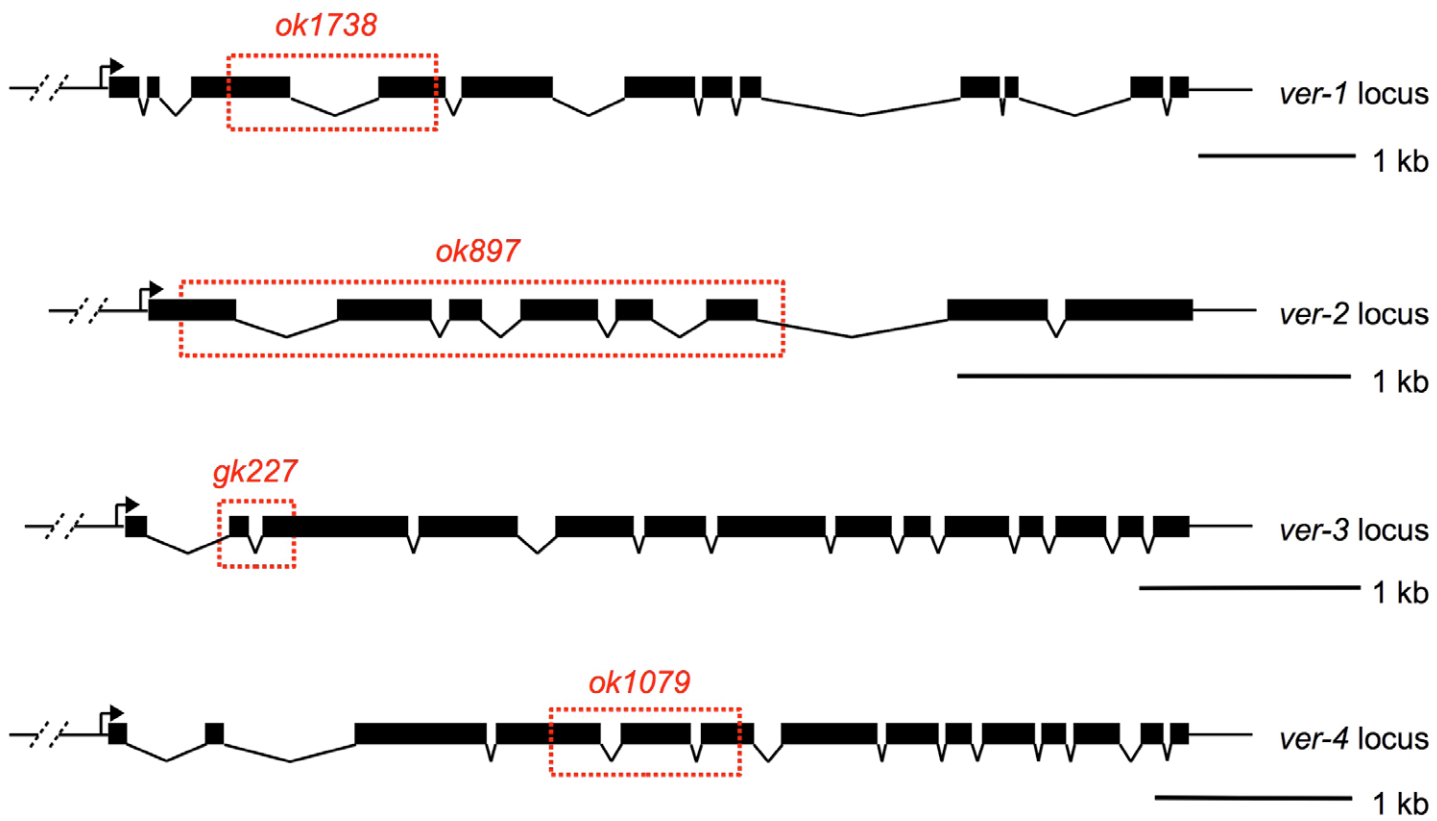
Fig. S1. The *ver* mutants. The predicted extent of deletions in the four *ver* mutants is shown.

Table S1. Raw data for Fig. 4

Strain	% DTC defects*	SE[‡]	n
1) *WT (him-5)*	0%	0%	110
2) *pvf-1(ev763)*	0%	0%	110
3) *plx-1(ev724)*	32%	4%	359
4) *pvf-1(ev763); plx-1(ev724)*	63%	4%	117
5) *pvf-1(ev763); plx-1(ev724); evEx429[pvf-1p::pvf-1(+)]*	21%	3%	143
6) *pvf-1(ev763); plx-1(ev724); evEx430[myo-3p::pvf-1(+)]*	34%	4%	150
7) *pvf-1(ev763); plx-1(ev724); evEx432[hsp16.41p:: pvf-1(+)] no HS[§]*	63%	4%	146
8) *pvf-1(ev763); plx-1(ev724); evEx432[hsp16.41p:: pvf-1(+)] HS[§]*	31%	4%	145
9) *pvf-1(ev763); plx-1(ev724); evEx430[myo-3p::mVEGF164]*	32%	4%	125
10) *unc-6(ev400)*	59%	3%	222
11) *pvf-1(ev763); unc-6(ev400)*	31%	2%	462
12) *pvf-1(ev763); unc-6(ev400); evEx433[pvf-1p::pvf-1(+)]*	63%	5%	104
13) *unc-40(e1430); pvf-1(ev763); unc-6(ev400)*	65%	3%	222
14) *unc-40(e1430)*	60%	3%	290
15) *unc-40(e1430); pvf-1(ev763)*	57%	3%	278
16) *unc-40(e1430); plx-1(ev724)*	98%	1%	130
17) *plx-1(ev724)*	32%	4%	359
18) *evIs103[unc-40p::unc-40gfp]*	51%	3%	248
19) *plx-1(ev724); evIs103*	96%	2%	92
20) *unc-6(ev400); evIs103*	24%	4%	103
21) *unc-6(ev400); evIs103/+*	41%	4%	96
22) *unc-5(e53); pvf-1(ev763); unc-6(ev400)*	50%	3%	311
23) *unc-5(e53)*	3%	1%	157
24) *pvf-1(ev763); unc-5(e53)*	4%	2%	155
25) *plx-1(ev724); unc-5(e53)*	71%	3%	180
26) *pvf-1(ev763); plx-1(ev724); unc-5(e53)*	67%	4%	167

*Proportion of male tail right and left sides with a severe ray 1 anterior defect.
[‡]Standard error of the proportion.
[§]Heat shock

Table S2. Raw data for Fig. 5

Strain	%DTC defects*	SE‡	*n*
1) *WT (him-5)*	0%	0%	110
2) *mig-2(mu28)*	2%	1%	185
3) *ced-10(n1993)*	1%	1%	297
4) *plx-1(ev724)*	32%	4%	359
5) *mig-2(mu28); plx-1(ev724)*	54%	3%	312
6) *plx-1(ev724); ced-10(n1993)*	70%	4%	128
7) *pvf-1(ev763)*	0%	0%	130
8) *pvf-1(ev763); ced-10(n1993)*	2%	1%	100
9) *mig-2(mu28); pvf-1(ev763)*	55%	5%	103
10) *unc-6(ev400)*	59%	3%	222
11) *unc-6(ev400); pvf-1(ev763)*	31%	2%	462
12) *unc-6(ev400); pvf-1(ev763); ced-10(n1993)/+*	49%	4%	141
13) *evEx434[ram-5p::ced-10(G12V)]*	0%	0%	112
14) *plx-1(ev724); evEx434*	79%	5%	76
15) *unc-6(ev400); evEx434*	12%	3%	93

*Proportion of male tail right and left sides with a severe ray 1 anterior defect.
‡Standard error of the proportion.

Table S3. Raw data for Fig. 6

Strain	%DTC defects*	SE‡	*n*
1) *WT (him-5)*	0%	0%	110
2) *ver-1(ok1738)*	1%	1%	138
3) *ver-2(ok897)*	0%	0%	120
4) *ver-3(gk227)*	0%	0%	115
5) *ver-4(ok1079)*	0%	0%	121
6) *plx-1(ev724)*	32%	4%	359
7) *pvf-1(ev763)*	0%	0%	130
8) *pvf-1(ev763); plx-1(ev724)*	63%	4%	117
9) *ver-1(ok1738); plx-1(ev724)*	57%	3%	203
10) *ver-2(ok897); plx-1(ev724)*	57%	4%	200
11) *ver-3(gk227); plx-1(ev724)*	66%	4%	116
12) *ver-4(ok1079); plx-1(ev724)*	60%	5%	103
13) *ver-1(ok1738); unc-6(ev400)*	31%	4%	118
14) *ver-2(ok897); unc-6(ev400);*	27%	3%	314
15) *ver-4(ok1079); unc-6(ev400);*	36%	4%	162
16) *unc-6(ev400)*	59%	3%	222
17) *unc-6(ev400); pvf-1(ev763)*	31%	2%	462
18) *ver-1(ok1738) pvf-1(ev763); plx-1(ev724)*	58%	4%	141
19) *ver-1(ok1738); plx-1(ev724); evEx437[lin-32p::ver-1(+)]*	23%	4%	114
20) *ver-1(ok1738); plx-1(ev724); evEx435[lin-32p::hKDR]*	29%	5%	96
21) *ver-1(ok1738); plx-1(ev724); evEx436[lin-32p::hFLT]*	37%	5%	115

*Proportion of male tail right and left sides with a severe ray 1 anterior defect.
‡Standard error of the proportion.